

# Strongly anisotropic vortices in dipolar quantum droplets

Guilong Li<sup>1</sup>, Zibin Zhao<sup>1</sup>, Xunda Jiang<sup>1</sup>, Zhaopin Chen<sup>2</sup>, Bin Liu<sup>1,\*</sup>, Boris A. Malomed<sup>3,4</sup>, and Yongyao Li<sup>1,5†</sup>

<sup>1</sup>*School of Physics and Optoelectronic Engineering, Foshan University, Foshan 528225, China*

<sup>2</sup>*Physics Department and Solid-State Institute, Technion, Haifa 32000, Israel*

<sup>3</sup>*Department of Physical Electronics, School of Electrical Engineering, Faculty of Engineering, Tel Aviv University, Tel Aviv 69978, Israel*

<sup>4</sup>*Instituto de Alta Investigación, Universidad de Tarapacá, Casilla 7D, Arica, Chile*

<sup>5</sup>*Guangdong-Hong Kong-Macao Joint Laboratory for Intelligent Micro-Nano Optoelectronic Technology, Foshan University, Foshan 528225, China*

We construct strongly anisotropic quantum droplets with embedded vorticity in the 3D space, with mutually perpendicular vortex axis and polarization of atomic magnetic moments. Stability of these anisotropic vortex quantum droplets (AVQDs) is verified by means of systematic simulations. Their stability area is identified in the parametric plane of the total atom number and scattering length of the contact interactions. We also construct vortex-antivortex-vortex bound states and find their stability region in the parameter space. The application of a torque perpendicular to the vorticity axis gives rise to robust intrinsic oscillations or rotation of the AVQDs. The effect of three-body losses on the AVQD stability is considered too. The results show that the AVQDs can retain the topological structure (vorticity) for a sufficiently long time if the scattering length exceeds a critical value.

Quantum droplets (QDs), representing a novel form of quantum matter, have drawn much interest in recent years [1–17]. These are droplets of an ultra-dilute superfluid maintained by the balance between the mean-field (MF) and beyond-MF effects [18, 19], the latter one being the Lee-Huang-Yang (LHY) correction [20, 21] to the MF nonlinearity induced by quantum fluctuations. QDs have been experimentally observed in dipolar Bose-Einstein condensates (BECs) [22, 23], as well as in binary BECs of nonmagnetic atoms, with quasi-2D [24, 25] and 3D [26–28]. On the contrary to that, experimental realization of self-trapped BECs in free space solely through MF effect is impossible due to the critical or supercritical collapse instability in the 2D and 3D settings, respectively [29–32] (nevertheless, weakly unstable quasi-2D *Townes solitons* were experimentally created in a binary BEC [33, 34]). 3D QDs in nonmagnetic condensates appear in the isotropic form, whereas their shapes are anisotropic in dipolar BECs [35, 36] (a possibility to create stable isotropic QDs in a 2D dipolar BEC was considered too [37]). Note that stable anisotropic quasi-2D fundamental (zero-vorticity) MF solitons (in the absence of the LHY correction) can be created in the magnetic BEC with the in-plane dipole polarization [38], but they do not exist in the 3D form [39].

QDs are the subject of a vast research area, including Monte-Carlo simulations [40–42], collective excitations [43–45], supersolids, [46–51], Borromean droplets [52], etc. A particularly interesting direction of the studies is embedding vorticity into the self-bound QDs. It is well known that the creation of self-trapped vortices in the multi-dimensional space is a challenging issue. The

azimuthal instability, which is induced by the underlying self-attraction, tends to split the 2D vortex ring or 3D torus (“donut”) into fragments [53–57]. This instability develops faster than the collapse driven by the self-attraction. In QDs, the splitting instability may be arrested by the competition between the MF attraction and LHY self-repulsion, similar to the stabilizing effect of the cubic-quintic nonlinearity in optics [55–58]. Stable vortex QDs with the winding numbers (topological charge) up to 5 and 2 (at least) were predicted in 2D [59] and 3D geometries [60], respectively. Stable semi-discrete vortex QDs were predicted in arrays of one-dimensional traps [61]. These results indicate that the equilibrium state of the LHY-stabilized superfluid provides a versatile platform for the creation of the stable self-bound vortices [62].

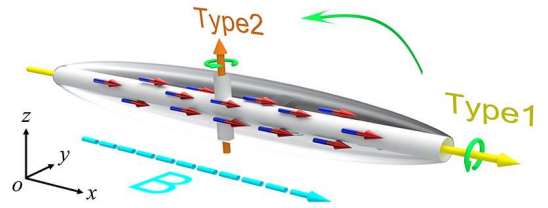


FIG. 1: Possible relations between the vorticity axis and polarization of atomic magnetic dipoles, which is fixed by magnetic field  $\mathbf{B}$  along the  $x$  axis. Type 1: the vorticity parallel to the polarization (the same as in Ref. [63]). This configuration is always unstable. Type 2: the new configuration, which may be stable, with the vorticity oriented perpendicular to the polarization.

The above-mentioned findings were produced for binary BECs of nonmagnetic atoms. For the dipolar QDs, isotropic vortex modes have been reported, with the vortex axis parallel to the polarization of atomic magnetic moments, represented by “Type 1” in Fig. 1. This con-

\*Electronic address: binliu@fosu.edu.cn

†Electronic address: yongyaoli@gmail.com

figuration is rotationally symmetric with respect to the vorticity axis, but it is known to be unstable [63]. The creation of *anisotropic* vortex QDs in dipolar BECs and their stability is a challenging problem. This problem is also relevant in studies of other nonlinear systems, as no example of anisotropic vortex solitons in free space was reported in any context. Very recently, stable vortex QDs were predicted in a 2D dipolar setup [64]. However, this problem was not previously addressed in the full 3D geometry.

In this Letter, we predict the existence of stable 3D strongly anisotropic vortex quantum droplets (3D-AVQDs) in the dipolar BEC with the magnetic dipoles polarized perpendicular to the vortex' axis, corresponding to the "Type 2" configuration in Fig. 1. Note that this configuration is not a straightforward extension of its 2D counterpart. In particular, the introduction of the third direction may readily give rise to flexural instability along the axis perpendicular to the plane of the original 2D mode, thus destroying the stability of the original 2D vortices. Moreover, the instability can also induce abundant new dynamics, such as the self-rotation along the dipole orientation, which does not exist in their 2D counterparts. Therefore, the stability of the 3D AVQDs is a challenging issue.

The respective 3D LHY-amended Gross-Pitaevskii equation (GPE) is written as

$$i\hbar \frac{\partial}{\partial t} \psi = -\frac{\hbar^2}{2m} \nabla^2 \psi + g|\psi|^2 \psi + \kappa \psi \int U_{\text{dd}}(\mathbf{r} - \mathbf{r}') |\psi(\mathbf{r}')|^2 d\mathbf{r}' + \gamma |\psi|^3 \psi + i\frac{\hbar}{2} \Lambda_3 |\psi|^4 \psi, \quad (1)$$

where  $\hbar$  and  $m$  are the Planck's constant and atomic mass,  $g = 4\pi\hbar^2 a_s/m$  with  $a_s$  being the  $s$ -wave scattering length of inter-atomic collisions, is the strength of the contact nonlinearity, which may be tuned by the Feshbach resonance [65, 66]. The coupling coefficient of the dipole-dipole interaction (DDI) is  $\kappa = \mu_0 \mu^2 / 4\pi$ , where  $\mu_0$  and  $\mu$  are the vacuum permeability and atomic magnetic moment of the atom. The coefficient in front of the LHY term is  $\gamma = \left(32ga_s^{3/2}/3\sqrt{\pi}\right) (1 + 3\epsilon_{\text{dd}}^2/2)$  [67–69], where the relative DDI strength  $\epsilon_{\text{dd}} \equiv a_{\text{dd}}/a_s$  is determined by the dipole scattering length,  $a_{\text{dd}} = \mu_0 \mu^2 m / 12\pi\hbar$  [22]. The DDI potential is  $U_{\text{dd}}(\mathbf{r} - \mathbf{r}') = (1 - 3\cos^2 \Theta) / |\mathbf{r} - \mathbf{r}'|^3$  [70, 71], where  $\cos^2 \Theta = (x - x')^2 / |\mathbf{r} - \mathbf{r}'|^2$ , and coefficient  $\lambda_3$  represents the three-body losses.

Disregarding the losses, the stationary solutions with chemical potential  $\Omega$  are looked for in the usual form,  $\psi(\mathbf{r}, t) = \phi(\mathbf{r})e^{-i\Omega t/\hbar}$ , with a stationary wave function  $\phi(\mathbf{r})$ . Equation (1) with  $\Lambda_3 = 0$  conserves the total atom number,  $N = \int |\psi(\mathbf{r})|^2 d\mathbf{r}$ , energy,  $E = \int d\mathbf{r} \left[ \frac{\hbar^2}{2m} |\nabla \psi|^2 + \frac{1}{2} g |\psi|^4 + \frac{1}{2} \kappa |\psi|^2 \int U_{\text{dd}}(\mathbf{r} - \mathbf{r}') |\psi(\mathbf{r}')|^2 d\mathbf{r}' + \frac{2}{5} \gamma |\psi|^5 \right]$ , and momentum (here we consider quiescent modes, with zero momentum).

3D-AVQD solutions with integer vorticity  $S$  can be produced in the numerical form by means of

the imaginary-time-integration method [72–74], initiated with an anisotropic input,

$$\phi^{(0)}(x, y, z) = A \tilde{r}^S \exp\left(-\alpha_1 \tilde{r}^2 - \alpha_2 z^2 + iS\tilde{\theta}\right), \quad (2)$$

where  $A$  and  $\alpha_{1,2}$  are positive real constants which determine widths of the input, and the deformed polar coordinates in the  $(x, y)$  plane are  $\{\tilde{r}, \tilde{\theta}\} \equiv \left\{ \sqrt{x^2 + \beta^2 y^2}, \arctan(\beta y/x) \right\}$  with an anisotropy factor  $\beta > 1$ . In this work, we select parameters of the BEC of dysprosium,  $^{164}\text{Dy}$ , which has a significant dipole scattering length,  $a_{\text{dd}} = 131a_0$  ( $a_0$  is the Bohr radius) [22]. The control parameters of the system are  $N$  and  $a_s$ .

The stability of the numerically obtained 3D-AVQDs solutions of Eq. (1) with  $S = 1$  was tested by real-time simulations of the perturbed evolution. The numerically found stability area for them in the  $(N, a_s)$  plane is plotted in Fig. 2(a), with a typical example of a stable 3D-AVQD shown in Fig. 2(b). The average atomic density of this state is  $140 \times 10^{20}$  atoms/m<sup>3</sup>, in agreement with the estimate in Ref [75]. In the simulations, stable 3D-AVQDs, which populate the blue areas in Fig. 2(a), maintain their integrity during a sufficient long time (at least,  $\sim 100$  ms), which is longer than the levitation time ( $\sim 90$  ms) in the experiment [22]. On the other hand, the unstable 3D-AVQDs [in the gray area in Fig. 2(a)] spontaneously transform into ground-state QDs after a few milliseconds. It is thus observed that 3D-AVQDs exist at  $a_s > 12a_0$ , and they are stable at  $a_s > 27a_0$ .

In the 2D geometry, particular *stable* bound-states with a vortex-antivortex-vortex structure were revealed [64]. Remarkably, similar bound-states can be created in the current 3D setting too, by means of input

$$\begin{aligned} \phi^{(0)} = & \sum_{+,-} A_{\pm} \tilde{r}_{\pm} \exp\left(-\alpha_1 \tilde{r}_{\pm}^2 - \alpha_2 z^2 + i\tilde{\theta}_{\pm}\right) \\ & + A\tilde{r} \exp\left(-\alpha_1 \tilde{r}^2 - \alpha_2 z^2 - i\tilde{\theta}\right). \end{aligned} \quad (3)$$

Here,  $A_{\pm} > 0$  and  $\alpha_{1,2} > 0$  are real constants,  $\tilde{r}_{\pm} \equiv \sqrt{(x \pm x_0)^2 + \beta^2 y^2}$ ,  $\tilde{\theta}_{\pm} \equiv \arctan[\beta y/(x \pm x_0)]$ , and  $x_0$  is an appropriately chosen separation, cf. Eq. (2). A typical example of such a stable composite QD with average density  $200 \times 10^{20}$  atoms/m<sup>3</sup> is displayed in Fig. 2(c). They are stable in the orange area in the plane of  $(N, a_s)$ , which is embedded in the broader stability region of the regular 3D-AVQDs, see Fig. 2(a). It is seen that the stable three-pivot vortex bound-states exist in the region of  $30 < a_s/a_0 < 45$  and  $1800 < N < 6400$ .

As mentioned above, the vortex states with the vorticity axis parallel to the polarization of the dipoles [see "Type 1" in Fig. 1] are completely unstable. Because these solutions are axially symmetric, they are marked SYM in Fig. 3. The 3D-AVQD solutions obtained here are anisotropic, therefore they are marked by the ASY label. Figure 3 displays the comparison of the total energy between the isotropic and anisotropic species of the vortex solutions. The energy of the fundamental (zero-vorticity) QDs, marked by FUND, is also included, as a

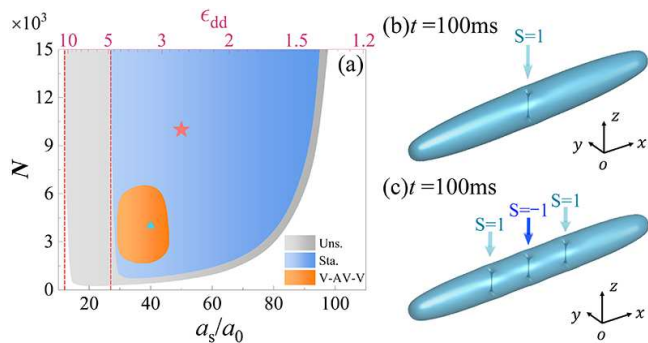


FIG. 2: (a) The areas of stable and unstable 3D-AVQDs, as well as stable vortex-antivortex-vortex bound-states in the plane of  $(N, a_s)$ , which populate the blue, gray and orange areas, respectively. The left dashed vertical line, at  $a_s = 12a_0$ , is the existence boundary for the 3D-AVQDs, and the right vertical line, at  $a_s = 27a_0$ , is their stability boundary. Red-font numbers, attached to the upper axis, are values of  $\epsilon_{dd}$ . (b-c) Typical examples of a stable 3D-AVQD and vortex-antivortex-vortex bound state with  $(N, a_s) = (10^4, 50a_0)$  and  $(4000, 40a_0)$ , corresponding to the red star and blue triangle, respectively, in panel (a). They survive the perturbed evolution in the course of 100 ms, at least.

reference. Figures 3(a,b) show that the unstable SYM vortex QDs have the highest energy (which is a natural explanation for their instability), while stable ASY vortex states have a lower energy, which is almost identical to that of the fundamental QDs.

For the SYM type of the vortex QDs, the void around the long axis implies the removal of a long tube filled by dipoles chiefly featuring attractive DDIs, i.e., the removal of the negative interaction energy, which causes them to have higher actual energy values, in accordance with Fig. 3(a,b). A typical example of the evolution of the SYM vortex-QD is displayed in Fig. 3(c1-c3), which demonstrates the instability-induced splitting. These results agree with the instability of the isotropic vortex solitons that was reported in Ref. [63]. On the other hand, the stability of the ASY type is feasible because the corresponding axial void removes a tube filled by dipoles chiefly featuring repulsive DDIs with the positive energy, thus producing lower actual energy values, as corroborated by Fig. 3(a,b). Additional analysis has demonstrated that the application of the imaginary-time-integration method to Eq. (1) does not generate 3D-AVQD solutions with multiple vorticity,  $S \geq 2$ .

To present systematic results for the 3D-AVQDs, we define their ellipticity  $\mathcal{A}$  and normalized angular momentum  $\bar{L}_z$ :

$$\mathcal{A} = \frac{D_S}{D_L}, \quad \bar{L}_z = \int \frac{\phi^* \hat{L}_z \phi}{N} d\mathbf{r}, \quad (4)$$

where  $D_S$  and  $D_L$  are, respectively, the short and long axes of the QDs, and  $\hat{L}_z = i\hbar(y\partial_x - x\partial_y)$  is the operator of the  $z$  components of the angular momentum. Dependences of the chemical potential, ellipticity, and angular

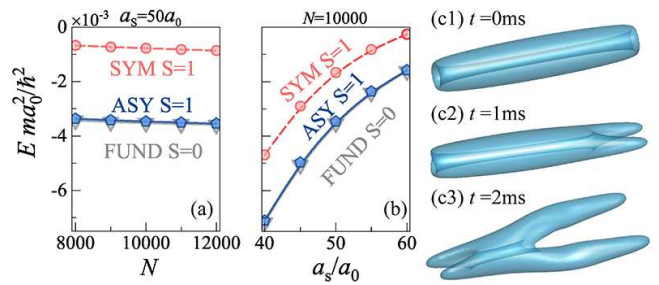


FIG. 3: (a-b) The total energy ( $E$ ) of the fundamental QDs (the grey curve labeled FUND), 3D-AVQDs (the blue curve labeled ASY), and isotropic vortical QDs (the red curve labeled SYM) versus  $N$  (a) and  $a_s$  (b). (c1-c3) The unstable evolution of a SYM vortex QD with  $(N, a_s) = (10^4, 50a_0)$  illustrated by its density profiles at  $t = 0$  ms, 1 ms, and 2 ms, respectively.

momentum on the number of atoms, for two different values of  $a_s$ , are produced in Fig. 4.

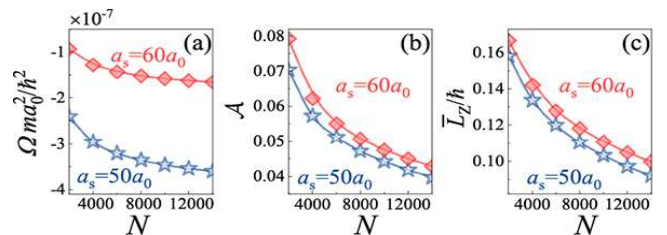


FIG. 4: (a) The chemical potential ( $\Omega$ ), (b) ellipticity ( $\mathcal{A}$ ), and (c) angular momentum ( $\bar{L}_z$ ) (see Eq. (4)) versus  $N$ , for  $a_s = 50a_0$  and  $60a_0$  (the chains of blue stars and red rhombuses, respectively).

In Fig. 4(a), the chemical potential  $\Omega$  satisfies the Vakhitov-Kokolov criterion,  $d\Omega/dN < 0$ , which is the well-known necessary stability condition for self-trapped modes [30, 76]. A basic feature of QDs is their incompressibility. This implies that the average density of the droplets cannot exceed a maximum value [18], which leads to flat-top QDs' shape. Thus, the volume of the QDs increases linearly with the growth of the number of atoms. Further, due to the strong DDI anisotropy, the increase of the volume is mostly represented by the extension along the  $x$ -axis, leading to the decrease of the ellipticity [see Eq. (4)] in Fig. 4(b). As the internal vorticity is mainly concentrated at the center of the droplet, Fig. 4(c) shows that larger values of norm correspond to longer droplets and lower values of the angular momentum. Moreover, figures 4(b,c) reveal that  $\bar{L}_z/\hbar = 2\mathcal{A}$ , which coincides with the relation found for strongly anisotropic 2D-AVQDs [64].

The shape of the 3D-AVQDs suggests a possibility to set it in rotation around an axis perpendicular to the vorticity vector. To this end, a torque was applied around the  $x$ -axis, multiplying the established 3D-AVQD by the phase factor  $\exp[i(z/z_0) \tanh(y/y_0)]$ , i.e., adding an  $x$ -

component of the angular momentum to the original  $z$ -component, cf. Ref. [77]. Here,  $z_0$  and  $y_0$  are length scales, which define the strength of the torque. Simulations reveal oscillations or rotation of the 3D-AVQDs around the  $x$ -axis, depending on values of  $z_0$  and  $y_0$ . The weak torque, corresponding to large ( $z_0$  and  $y_0$ ), induces oscillations, whose period increases with the decrease of  $z_0$  and  $y_0$ . Divergence of the oscillation period implies a transition to the rotation, caused by a sufficiently strong torque (see Movies I and II in Supplemental Material). The rotation speed increases with the further decrease of  $y_0$  and  $z_0$ , as the torque is made still stronger. Figure 5(a) displays the oscillation and rotation regions in the plane of  $(z_0^{-1}, y_0)$  for  $(N, a_s) = (10^4, 50a_0)$ . The border between these dynamical regimes is fitted by  $y_0 = Z_0^2/z_0 + Y_0$ , with  $Z_0 \approx 0.88 \mu\text{m}$  and  $Y_0 \approx 0.06 \mu\text{m}$ . This relation is explained by the fact that, for  $|y| \lesssim y_0$ , the torque's phase,  $\approx yz/(y_0z_0)$ , is determined solely by product  $y_0z_0$ . Periods of the oscillations and rotation are displayed, as functions of  $z_0^{-1}$ , by insets in the respective regions. A typical example of the stable rotation is presented in Fig. 5(b1-b3). The rotation picture is the same as produced by the stationary solution of Eq. (1) in the rotating reference frame, which includes term  $\omega \hat{L}_x \psi$ , where  $\hat{L}_x = i\hbar(z\partial_y - y\partial_z)$  and  $\omega$  is the rotation frequency.

We have also explored results of the application of the torque around the  $y$ - and  $z$ -axes, in terms of Fig. 1. In the former case, the torque drives a complex dynamical regime: the prolate QD features oscillations in the  $(z, x)$  plane, simultaneously with irregular rotation around the  $x$  axis (not around the  $y$  direction), as shown by Movie III in Supplemental Material. Lastly, the application of a weak torque along the  $z$  direction initiates oscillations of the prolate vortex soliton in the  $(x, y)$  plane (see Movie IV in Supplemental Material), while a stronger torque leads to its splitting, the boundary between the two regimes being  $x_0 = Y_0^2/y_0 + X_0$ , where  $Y_0 \approx 0.67 \mu\text{m}$  and  $X_0 \approx -0.5 \mu\text{m}$ , in terms of the torque's spatial scales.

Finally, it is imperative to consider the effect of three-body losses, characterized by coefficient  $\Lambda_3 = 1.25 \times 10^{-41} \text{m}^6\text{s}^{-1}$  in Eq. (1) [22]. In general, losses may attenuate instabilities for fundamental (zero-vorticity) states, but this is not applicable to vortex QDs, whose stability is determined by the equilibrium value of the density. We observe that the scattering length  $a_s$  significantly affects the loss effect. Notably, for  $N = 10^4$ , if  $a_s$  is smaller than a critical value,  $66a_0$ , the losses drive rapid degeneration of the initial vortex QD into a fundamental (zero-vorticity) state in the course of  $< 100$  ms (see Movie V in Supplemental Material). The residual state survives much longer, which implies that the QD's topological structure is especially vulnerable to the loss effect. However, at  $a_s > 66a_0$ , the robustness is much improved. For example, as shown in Fig. 6(a-c), the vortex-QD with  $a_s = 70a_0$  retains its topological charge for more than 400 ms (see Movie VI in Supplemental Material). As shown in Fig. 6(d), in the latter case the total atom number  $N$ ,

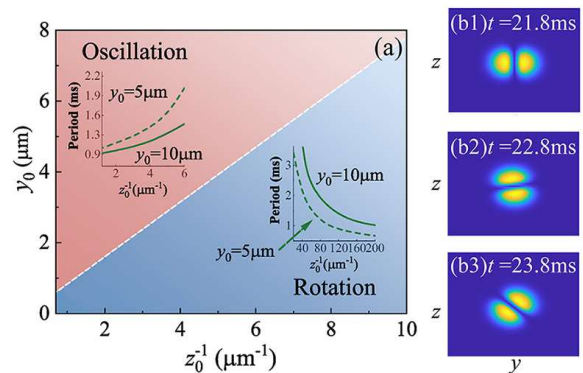


FIG. 5: (a) The oscillation and rotation regions in the plane of the torque's parameters, for  $(N, a_s) = (10^4, 50a_0)$ . The insets show the oscillation and rotation periods vs.  $z_0^{-1}$  for fixed  $y_0 = 5$  and  $10 \mu\text{m}$  (the dashed and solid lines, respectively). (b1-b3) Plots of the cross-section density in the  $(y, z)$  plane illustrating the robust rotation of the 3D-AVQD around the  $x$ -axis, with period 5.5 ms, initiated by the torque with  $(z_0, y_0) = (0.05, 5) \mu\text{m}$ .

effective volume  $V = (\int |\psi|^2 d\mathbf{r})^2 / \int |\psi|^4 d\mathbf{r}$ , and density  $\rho = N/V$  of the QD decrease slowly, demonstrating that the losses are not a fatal factor.

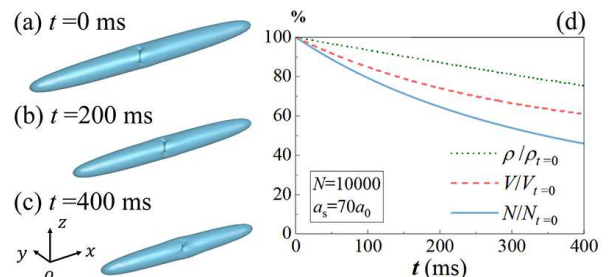


FIG. 6: (a-c) The real-time evolution of the droplet with three-body losses for  $N = 10^4$  and  $a_s = 70a_0$ . (d) The residual ratio of  $N$ ,  $V$ , and  $\rho$  vs. time.

*Conclusion* We have predicted the existence of stable AVQDs (anisotropic vortex quantum droplets) in 3D dipolar BECs, with the strong anisotropy imposed by the orthogonality of the vorticity and polarization of atomic magnetic moments. While isotropic vortex solitons in dipolar BEC are completely unstable, we have identified a vast stability region of 3D-AVQDs in the system's parameter space. The existence of stable composite states with the vortex-antivortex-vortex structure is demonstrated as well, and their stability area is identified. Essential characteristics of the 3D AVQDs, including the chemical potential, aspect ratio, and angular momentum, are presented as functions of control parameters. Furthermore, we have demonstrated that the application of the torque perpendicular to the vorticity axis initiates robust intrinsic oscillations or rotation of the 3D-AVQDs. The dependence of the oscillation and rotation periods on parameters of the torque have been found. The persis-

tence of the 3D-AVQDs under the action of three-body losses was analyzed too, demonstrating that the topological structure (vorticity) is retained by the 3D AVQD for a sufficiently long time when the scattering length exceeds a critical value.

As an extension of the present analysis, it may be relevant to look for more complex bound states of AVQDs, and to study a two-component version of the model, cf. Refs. [78–80]. Another relevant problem is to add an ingredient (probably, an external potential) that may help to stabilize higher-order anisotropic vortex solitons, with  $S \geq 2$ .

### Acknowledgments

Authors appreciate valuable discussions with Profs. Zhenya Yan, G. E. Astrakharchik, Yongchang Zhang,

and Dr. Xizhou Qin. This work was supported by NNSFC (China) through Grants No. 12274077, 12305013, 11874112, 11905032, the Natural Science Foundation of Guangdong province through Grant No. 2024A1515030131, 2023A1515010770, the Research Fund of Guangdong-Hong Kong-Macao Joint Laboratory for Intelligent Micro-Nano Optoelectronic Technology through grant No.2020B1212030010. The work of B.A.M. is supported, in part, by the Israel Science Foundation through grant No. 1695/22.

- 
- [1] I. Ferrier-Barbut and T. Pfau, Quantum Liquids Get Thin, *Science* **359**, 274 (2018).
- [2] M. Guo and T. Pfau, A new state of matter of quantum droplets, *Front. Phys.* **16**, 32202 (2021).
- [3] Z. Luo, W. Pang, B. Liu, Y. Li, and B. A. Malomed, A new kind form of liquid matter: Quantum droplets, *Front. Phys.* **16**, 32201 (2021).
- [4] B. A. Malomed, The family of quantum droplets keeps expanding, *Front. Phys.* **16**, 22504 (2021).
- [5] F. Böttcher, J.-N. Schmidt, J. Hertkorn, K. S. H. Ng, S. D. Graham, M. Guo, T. Langen, and T. Pfau, New States of Matter with Fine-Tuned Interactions: Quantum Droplets and Dipolar Supersolids, *Rep. Prog. Phys.* **84**, 012403 (2021).
- [6] L. Chomaz, I. Ferrier-Barbut, F. Ferlaino, B. Laburthe-Tolra, B. L. Lev, and T. Pfau, Dipolar Physics: A Review of Experiments with Magnetic Quantum Gases, *Rep. Prog. Phys.* **86**, 026401 (2023).
- [7] I. Ferrier-Barbut, M. Schmitt, M. Wenzel, H. Kadau, and T. Pfau, Liquid Quantum Droplets of Ultracold Magnetic Atoms, *J. Phys. B: At. Mol. Opt. Phys.* **49**, 214004 (2016).
- [8] G. E. Astrakharchik and B. A. Malomed, Dynamics of one-dimensional quantum droplets, *Phys. Rev. A* **98**, 013631 (2018).
- [9] T. G. Skov, M. G. Skou, N. B. Jørgensen, and J. J. Arlt, Observation of a Lee-Huang-Yang Fluid, *Phys. Rev. Lett.* **126**, 230404 (2021).
- [10] Y.-C. Xiong and L. Yin, Self-Bound Quantum Droplet with Internal Stripe Structure in 1D Spin-Orbit-Coupled Bose Gas, *Chinese Phys. Lett.* **38**, 070301 (2021).
- [11] F. Zhang and L. Yin, Phonon Stability of Quantum Droplets in Dipolar Bose Gases, *Chinese Phys. Lett.* **39**, 060301 (2022).
- [12] Y. Wang, L. Guo, S. Yi, and T. Shi, Theory for Self-Bound States of Dipolar Bose-Einstein Condensates, *Phys. Rev. Research* **2**, 043074 (2020).
- [13] T. A. Yoğurt, U. Tanyeri, A. Keleş and M. Ö. Oktel, Vortex Lattices in strongly confined quantum droplets, *Phys. Rev. A* **108**, 033315 (2023).
- [14] A. Yang, J. Zhou, X. Liang, G. Li, B. Liu, H.-B. Luo, B. A. Malomed, and Y. Li, Two-Dimensional Quantum Droplets in Binary Quadrupolar Condensates, *New J. Phys.* **26**, 053037 (2024).
- [15] L. Dong and Y. V. Kartashov, Rotating Multidimensional Quantum Droplets, *Phys. Rev. Lett.* **126**, 244101 (2021).
- [16] H. Zhu, Y.-Q. Ma, W.-K. Bai, Y.-M. Yu, F.-F. Ye, Y.-Y. Li, L. Zhuang, and W.-M. Liu, Three-Dimensional Isotropic Droplets in Rydberg-Dressed Bose Gases, *Phys. Rev. Research* **6**, 023151 (2024).
- [17] E. A. L. Henn, Quantum Vortices Get Stretched, *Front. Phys.* **19**, 31301 (2024).
- [18] D. S. Petrov, Quantum Mechanical Stabilization of a Collapsing Bose-Bose Mixture, *Phys. Rev. Lett.* **115**, 155302 (2015).
- [19] D. S. Petrov and G. E. Astrakharchik, Ultradilute Low-Dimensional Liquids, *Phys. Rev. Lett.* **117**, 100401 (2016).
- [20] T. D. Lee, K. Huang, and C. N. Yang, Eigenvalues and eigenfunctions of a Bose system of hard spheres and its low-temperature properties, *Phys. Rev.* **106**, 1135-1145 (1957).
- [21] N. B. Jørgensen, G. M. Bruun, and J. J. Arlt, Dilute Fluid Governed by Quantum Fluctuations, *Phys. Rev. Lett.* **121**, 173403 (2018).
- [22] M. Schmitt, M. Wenzel, F. Böttcher, I. Ferrier-Barbut, and T. Pfau, Self-bound droplets of a dilute magnetic quantum liquid, *Nature* **539**, 259 (2016).
- [23] L. Chomaz, S. Baier, D. Petter, M. J. Mark, F. Wächtler, L. Santos, and F. Ferlaino, Quantum-Fluctuation-Driven Crossover from a Dilute Bose-Einstein Condensate to a Macrodroplet in a Dipolar Quantum Fluid, *Phys. Rev. X* **6**, 041039 (2016).
- [24] C. R. Cabrera, L. Tanzi, J. Sanz, B. Naylor, P. Thomas, P. Cheiney, and L. Tarruell, Quantum Liquid Droplets in a Mixture of Bose-Einstein Condensates, *Science* **359**, 301 (2018).
- [25] P. Cheiney, C. R. Cabrera, J. Sanz, B. Naylor, L. Tanzi, and L. Tarruell, Bright soliton to quantum droplet tran-

- sition in a mixture of Bose-Einstein condensates, *Phys. Rev. Lett.* **120**, 135301 (2018).
- [26] G. Semeghini, G. Ferioli, L. Masi, C. Mazzinghi, L. Wolswijk, F. Minardi, M. Modugno, G. Modugno, M. Inguscio, and M. Fattori, Self-Bound Quantum Droplets of Atomic Mixtures in Free Space, *Phys. Rev. Lett.* **120**, 235301 (2018).
- [27] G. Ferioli, G. Semeghini, L. Masi, G. Giusti, G. Modugno, M. Inguscio, Albert Gallemí, A. Recati, and M. Fattori, Collisions of Self-Bound Quantum Droplets, *Phys. Rev. Lett.* **122**, 090401 (2019).
- [28] C. D’Errico, A. Burchianti, M. Prevedelli, L. Salasnich, F. Ancilotto, M. Modugno, F. Minardi, and C. Fort, Observation of quantum droplets in a heteronuclear bosonic mixture, *Phys. Rev. Res.* **1**, 033155 (2019).
- [29] G. Fibich and G. Papanicolaou, Self-focusing in the perturbed and unperturbed nonlinear Schrödinger equation in critical dimension, *SIAM J. Appl. Math.* **60**, 183 (1999).
- [30] L. Bergé, Wave collapse in physics: principles and applications to light and plasma waves, *Phys. Rep.* **303**, 259 (1998).
- [31] E. A. Kuznetsov and F. Dias, Bifurcations of solitons and their stability, *Phys. Rep.* **507**, 43 (2011).
- [32] C. Pethick and H. Smith, *Bose-Einstein Condensation in Dilute Gases* (Cambridge University Press, Cambridge; New York, 2002).
- [33] C.-A. and C.-L. Hung, Observation of universal quench dynamics and Townes soliton formation from modulational instability in two-dimensional Bose gases, *Phys. Rev. Lett.* **125**, 250401 (2020).
- [34] B. Bakkali-Hassani, C. Maury, Y.-Q. Zhou, E. Le Cerf, R. Saint-Jalm, P. C. M. Castilho, S. Nascimbene, J. Dalibard, and J. Beugnon, Realization of a Townes Soliton in a Two-Component Planar Bose Gas, *Phys. Rev. Lett.* **127**, 023603 (2021).
- [35] D. Baillie, R. M. Wilson, R. N. Bisset, and P. B. Blakie, Self-Bound Dipolar Droplet: A Localized Matter Wave in Free Space, *Phys. Rev. A* **94**, 021602 (2016).
- [36] M. Wenzel, F. Böttcher, J.-N. Schmidt, M. Eisenmann, T. Langen, T. Pfau, and I. Ferrier-Barbut, Anisotropic Superfluid Behavior of a Dipolar Bose-Einstein Condensate, *Phys. Rev. Lett.* **121**, 030401 (2018).
- [37] A. Boudjemaa, Two-dimensional quantum droplets in dipolar Bose gases, *New J. Phys.* **21**, 093027 (2019).
- [38] I. Tikhonenkov, B. A. Malomed, and A. Vardi, Anisotropic solitons in dipolar Bose-Einstein condensates, *Phys. Rev. Lett.* **100**, 090406 (2008).
- [39] T. Lahaye, J. Metz, B. Fröhlich, T. Koch, M. Meister, A. Griesmaier, T. Pfau, H. Saito, Y. Kawaguchi, and M. Ueda, *d*-Wave Collapse and Explosion of a Dipolar Bose-Einstein Condensate, *Phys. Rev. Lett.* **101**, 080401 (2008).
- [40] M. A. Garcia-March, B. Julia-Diaz, G. E. Astrakharchik, T. Busch, J. Boronat, and A. Polls, Quantum correlations and spatial localization in one-dimensional ultracold bosonic mixtures, *New J. Phys.* **16**, 103004 (2014).
- [41] L. Parisi, G. E. Astrakharchik, and S. Giorgini, Liquid State of One-Dimensional Bose Mixtures: A Quantum Monte Carlo Study, *Phys. Rev. Lett.* **122**, 105302 (2019).
- [42] V. Cikojević, L. V. Markić, M. Pi, M. Barranco, and J. Boronat, Towards a quantum Monte Carlo-based density functional including finite-range effects: Excitation modes of a  $^{39}\text{K}$  quantum droplet, *Phys. Rev. A* **102**, 033335 (2020).
- [43] M. Tylutki, G. E. Astrakharchik, B. A. Malomed, D. S. Petrov, Collective excitations of a one-dimensional quantum droplet, *Phys. Rev. A* **101**, 051601(R) (2020).
- [44] H. Hu, and X. Liu, Consistent Theory of Self-Bound Quantum Droplets with Bosonic Pairing, *Phys. Rev. Lett.* **125**, 195302 (2020).
- [45] D. Baillie, R. M. Wilson, and P. B. Blakie, Collective Excitations of Self-Bound Droplets of a Dipolar Quantum Fluid, *Phys. Rev. Lett.* **119**, 255302 (2017).
- [46] Y. Zhang, F. Maucher, and T. Pohl, Supersolidity around a Critical Point in Dipolar Bose-Einstein Condensates, *Phys. Rev. Lett.* **123**, 015301 (2019).
- [47] Y. Zhang, T. Pohl, and F. Maucher, Phases of supersolids in confined dipolar Bose-Einstein condensates, *Phys. Rev. A* **104**, 013310 (2021).
- [48] F. Böttcher, J.-N. Schmidt, M. Wenzel, J. Hertkorn, M. Guo, T. Langen, and T. Pfau, Transient Supersolid Properties in an Array of Dipolar Quantum Droplets, *Phys. Rev. X* **9**, 011051 (2019).
- [49] J. Hertkorn, J.-N. Schmidt, M. Guo, F. Böttcher, K. S. H. Ng, S. D. Graham, P. Uerlings, H. P. Büchler, T. Langen, M. Zwierlein, and T. Pfau, Supersolidity in Two-Dimensional Trapped Dipolar Droplet Arrays, *Phys. Rev. Lett.* **127**, 155301 (2021).
- [50] J. Sánchez-Baena, C. Politi, F. Maucher, F. Ferlaino, and T. Pohl, Heating a Dipolar Quantum Fluid into a Solid, *Nat. Commun.* **14**, 1868 (2023).
- [51] D. Scheiermann, L. A. P. Ardila, T. Bland, R. N. Bisset, and L. Santos, Catalyzation of Supersolidity in Binary Dipolar Condensates, *Phys. Rev. A* **107**, L021302 (2023).
- [52] Y. Ma, C. Peng, and X. Cui, Borromean Droplet in Three-Component Ultracold Bose Gases, *Phys. Rev. Lett.* **127**, 043002 (2021).
- [53] B. A. Malomed, Vortex solitons: Old results and new perspectives, *Physica D* **399**, 108 (2019).
- [54] B. A. Malomed, *Multidimensional Solitons* (American Institute of Physics: Melville, NY, 2022).
- [55] M. Quiroga-Teixeiro and H. Michinel, Stable azimuthal stationary state in quintic nonlinear optical media, *J. Opt. Soc. Am. B* **14**, 2004-2009 (1997).
- [56] R. L. Pego and H. A. Warchall, Spectrally stable encapsulated vortices for nonlinear Schrödinger equations, *J. Nonlinear Sci.* **12**, 347-394 (2002).
- [57] D. Mihalache, D. Mazilu, L.-C. Crasovan, I. Towers, A. V. Buryak, B. A. Malomed, L. Torner, J. P. Torres, and F. Lederer, Stable spinning optical solitons in three dimensions, *Phys. Rev. Lett.* **88**, 073902 (2002).
- [58] A. S. Reyna and C. B. de Araújo, High-order optical nonlinearities in plasmonic nanocomposites – a review, *Adv. Opt. Phot.* **9**, 720-774 (2017).
- [59] Y. Li, Z. Chen, Z. Luo, C. Huang, H. Tan, W. Pang, and B. A. Malomed, Two-dimensional vortex quantum droplets, *Phys. Rev. A* **98**, 063602 (2018).
- [60] Y. V. Kartashov, B. A. Malomed, L. Tarruell, and L. Torner, Three-Dimensional Droplets of Swirling Superfluids, *Phys. Rev. A* **98**, 013612 (2018).
- [61] X. Zhang, X. Xu, Y. Zheng, Z. Chen, B. Liu, C. Huang, B. A. Malomed, and Y. Li, Semidiscrete Quantum Droplets and Vortices, *Phys. Rev. Lett.* **123**, 133901 (2019).
- [62] Gui-hua Chen, Hong-cheng Wang, Hai-ming Deng, and B. A. Malomed, Vortex Quantum Droplets under Competing Nonlinearities, *Chinese Phys. Lett.* **41**, 020501

- (2024).
- [63] A. Cidrim, F. E. A. dos Santos, E. A. L. Henn, and T. Macrı, Vortices in self-bound dipolar droplets, *Phys. Rev. A* **98**, 023618 (2018).
- [64] G. Li, X. Jiang, B. Liu, Z. Chen, B. A. Malomed, and Y. Li, Two-Dimensional Anisotropic vortex quantum droplets in dipolar Bose-Einstein condensates, *Front. Phys.* **19**, 22202 (2024).
- [65] C. Chin, R. Grimm, P. Julienne, and E. Tiesinga, Feshbach Resonances in Ultracold Gases, *Rev. Mod. Phys.* **82**, 1225 (2010).
- [66] P. Courteille, R. S. Freeland, D. J. Heinzen, F. A. van Abeelen, and B. J. Verhaar, Observation of a Feshbach Resonance in Cold Atom Scattering, *Phys. Rev. Lett.* **81**, 69 (1998).
- [67] R. Schutzhold, M. Uhlmann, Y. Xu, and U. R. Fischer, Mean-field Expansion in Bose-Einstein Condensates with Finite-range Interactions, *Int. J. Mod. Phys. B* **20**, 3555 (2006).
- [68] A. R. P. Lima and A. Pelster, Quantum Fluctuations in Dipolar Bose Gases, *Phys. Rev. A* **84**, 041604 (2011).
- [69] F. Wachtler and L. Santos, Quantum Filaments in Dipolar Bose-Einstein Condensates, *Phys. Rev. A* **93**, 061603 (2016).
- [70] T. Lahaye, C. Menotti, L. Santos, M. Lewenstein, and T. Pfau, The Physics of Dipolar Bosonic Quantum Gases, *Rep. Prog. Phys.* **72**, 126401 (2009).
- [71] J. Stuhler, A. Griesmaier, T. Koch, M. Fattori, T. Pfau, S. Giovanazzi, P. Pedri, and L. Santos, Observation of Dipole-Dipole Interaction in a Degenerate Quantum Gas, *Phys. Rev. Lett.* **95**, 150406 (2005).
- [72] L. M. Chiofalo, S. Succi, and P. M. Tosi, Ground state of trapped interacting Bose-Einstein condensates by an explicit imaginary time algorithm, *Phys. Rev. E* **62**, 7438 (2000).
- [73] J. Yang and T. I. Lakoba, Accelerated imaginary-time evolution methods for the computation of solitary waves, *Stud. Appl. Math.* **120**, 265 (2008)
- [74] X. Antoine, W. Bao, and C. Besse, Computational methods for the dynamics of the nonlinear Schrodinger/Gross-Pitaevskii equations, *Comp. Phys. Commun.* **184**, 2621-2633 (2013).
- [75] I. Ferrier-Barbut, H. Kadau, M. Schmitt, M. Wenzel, and T. Pfau, Observation of Quantum Droplets in a Strongly Dipolar Bose Gas, *Phys. Rev. Lett.* **116**, 215301 (2016).
- [76] N. G. Vakhitov and A. A. Kolokolov, Stationary solutions of the wave equation in a medium with nonlinearity saturation, *Radiophys. Quantum Electron.* **16**, 783-789 (1973).
- [77] Y. V. Kartashov, B. A. Malomed, Y. Shnir, and L. Torner, Twisted Toroidal Vortex Solitons in Inhomogeneous Media with Repulsive Nonlinearity, *Phys. Rev. Lett.* **113**, 264101 (2014).
- [78] A. Boudjemaa, Fluctuations and quantum self-bound droplets in a dipolar Bose-Bose mixture, *Phys. Rev. A* **98**, 033612 (2018).
- [79] R. N. Bisset, L. A. P. Ardila, and L. Santos, Quantum Droplets of Dipolar Mixtures, *Phys. Rev. Lett.* **126**, 025301 (2021).
- [80] J. C. Smith, D. Baillie, and P. B. Blakie, Quantum Droplet States of a Binary Magnetic Gas, *Phys. Rev. Lett.* **126**, 025302 (2021).